International Journal of Engineering Research & Technology (IJERT)
ISSN: 2278-0181
Vol. 15 Issue 03 , March - 2026

Design and Performance Evaluation of Energy-Efficient Smart Streetlights in Rural Communities in Countries with Limited Resources

Seunghan Lee
Corresponding Author: SLee@STEMsc.org
Environmental Energy Divisions, STEM Science Center
111 Charlotte Place Ste#100/Englewood Cliffs, NJ 07632

ABSTRACT - Rationale: Many countries with limited resources suffer from persistent long-standing deficiencies in nighttime street lighting, particularly in rural and peri-urban communities where grid infrastructure is insufficient or unreliable. The absence of illumination intensifies traffic hazards, reduces walkability, and limits commercial activity after dusk, while perceived darkness can correlate with opportunity crimes and fear of being victims. Methods: This study reports the design, and engineering evaluation of a low-cost solar smart streetlight that integrates four vertically mounted photovoltaic panels combined in parallel connection for a 12 V battery subsystem, and an Arduino-based control unit for adaptive lighting. The study established two off-grid solar streetlight control architectures: a high-current Arduino Mega–based system and an ultra-low-power Arduino Nano 33 BLE Sense Rev2 system. Through a series of DI-256 instrumented recordings across the day–night cycles, the electrical behavior of both systems was analyzed, including battery voltage response, solar panel activation, Solar Charge Controller (SCC) mode transitions, MOSFET switching behavior, and PIR-triggered load activation. Results: It shows that the Mega system exhibits rapid nighttime battery depletion, SCC low-voltage lockouts, unstable MOSFET activation, and excessive energy consumption (~18.5 Wh per night) despite its promising functional expandability. In contrast, the Nano system demonstrates excellent nighttime survivability, extremely low energy consumption (~1.2 Wh), stable 5 V logic rail regulation, and clean MOSFET switching with minimal battery disturbance. The Nano architecture maintained full operational continuity through sunrise, dusk, and PIR events without instability. These findings establish the Nano-based design as a highly efficient, robust, and field-ready architecture suitable for solar lighting deployments. Further, simulated deployment demonstrated 35–45% energy savings relative to fixed-output systems while satisfying average illuminance targets and maintaining >10 h nighttime security under typical day-night insolation. Conclusion: This research demonstrates that sensor-controlled solar streetlights, engineered with budget components, can deliver reliable, energy-efficient lighting for underdeveloped areas and provide a replicable blueprint for broader deployment in data-underserved, resource-limited communities.

Keywords: Solar Smart Streetlight, Arduino-Based Control System, Energy Efficiency Optimization, Off-Grid Renewable Lighting, Low-Power Embedded Systems

INTRODUCTION

As a representative country with limited resources, Cambodia's rural communities face consistent infrastructural and environmental challenges that significantly limit their development [1]. Although the nation has rapidly progressed, its rural regions remain severely underdeveloped in terms of access to energy, lighting, and public safety infrastructure [2]. According to national energy and development reports, a large share of the Cambodian population continues to live in rural areas where electricity access remains incomplete or unreliable [3]. In many villages, households rely on small diesel generators, car batteries, or limited-capacity solar units that can provide only basic lighting for a few hours each night [4]. As a result, organized public street lighting is often absent, which can increase perceived insecurity and reduce safe evening mobility [5].

This lack of street lighting not only limits local productivity but also worsens quality of life after sunset [6]. Poor nighttime visibility on roads and pathways can increase the risk of accidents and exposure to environmental hazards [7]. In such settings, energy poverty and underdeveloped infrastructure reinforce each other by limiting education, commerce, and social activity during evening hours [8]. The core problem underlying rural darkness is the chronic shortage of dependable electrical infrastructure [9]. Many off-grid or weak-grid villages cannot support continuous outdoor lighting loads [10]. Even where small private lights exist, their output is usually insufficient to illuminate shared streets or community spaces [11]. Accordingly, low-cost public lighting systems remain an important infrastructure need in resource-limited communities [12].

International Journal of Engineering Research & Technology (IJERT)
ISSN: 2278-0181
Vol. 15 Issue 03 , March - 2026

Modern smart-lighting implementations often use microcontrollers such as Arduino, Raspberry Pi, or ESP32 together with passive infrared (PIR) or related sensors to detect motion and activate lighting only when needed [13]. This control strategy can reduce power consumption compared with continuously operated streetlights [14]. Sensor-triggered control is especially attractive for off-grid solar systems because it extends battery autonomy and improves nighttime survivability [15]. Despite these advantages, several issues hinder effective deployment in rural Southeast Asian settings [16]. First, cost and scalability remain major concerns because commercial smart-lighting products with communications features and advanced battery systems are often too expensive for small communities [17]. Second, harsh environmental conditions such as humidity, rainfall, dust, and heat can reduce component reliability and increase maintenance burden [18]. Third, inadequate charging control or poor energy budgeting can lead to battery over-discharge, shortened system lifetime, and seasonal instability [19].

During monsoon periods, reduced solar generation can coincide with continued nighttime lighting demand, making energy management even more critical [20]. In response to these limitations, this research proposes a low-cost, energy-efficient, and adaptive smart streetlight system based on microcontroller technology [21]. The system is designed to provide longer lighting hours while minimizing energy consumption through stricter activation conditions [22]. Its primary functions include motion-triggered illumination using a PIR sensor [23], ambient-light adjustment using an LDR for dusk and dawn transitions [24], solar-powered off-grid operation through a photovoltaic panel and rechargeable battery [25], and programmed energy-optimization logic to reduce unnecessary battery drain [26]. The design emphasizes simplicity and maintainability so that all major components—microcontroller, sensors, LED modules, and wiring—remain low cost and replaceable [27]. Installation requires only modest technical skill, making the system replicable across villages and small communities [28]. Moreover, the modular architecture allows future integration of data logging and user-behavior analysis for further energy-efficiency studies [29].

3. EXPERIMENTAL METHODS

3.1 Methods and Electrical Devices

Solar Panel: These are low-light performances. Each panel comes with 35-inch cables. Bypass diodes are pre-installed in a waterproof IP65 rated junction box to minimize power drop caused by shade and ensure excellent performance in low-light environments. Daily output reaches 1600wh under the condition of 4 hours of sunlight. PERC technology boosts cell efficiency to 23% by enhancing sunlight reflection, greatly improving sunlight utilization. Basic generator component for 12V/24V battery charging for on-grid, off-grid and hybrid power systems for home, garden, RV, Boat and agriculture.

Rechargeable Battery: Mighty Max Battery 12V 18AH SLA Replacement Battery for Powerland 10000 WATT Generator Brand Product. the mighty max ML18-12 12 volt 18 Ah uses a state of the art heavy-duty calcium-alloy grid that provides exceptional performance and service life in both float and cyclic applications. The ML18-12 is an absorbent glass mat (AGM) technology with a valve regulated design that can be used in enclosed and indoor environments without leaking or maintenance providing a superior performance for thousands of models.

Solar Charge Controller: With the built-in industrial microcontroller, this PWM solar charge controller automatically helps manage the working of solar panels and batteries in solar systems. When the battery runs out, it will memorize various parameters that are set, satisfying the need to reset it every time. The 30A solar charge controller is compatible with 12V or 24V systems automatically, only suitable for lead-acid batteries, such as OPEN, AGM, and GEL. Dual USB 5V/3A output ports support mobiles, tablet PCs, or other devices that require 5V voltage. It is easy to read the status and data with an LCD display, which is also able to switch modes and parameter configuration, such as adjustment of battery float, reconnect, and stop discharge voltage, which can perfectly protect the battery from over-discharge. The built-in overcurrent protection, short circuit protection, reverse connection protection, open circuit protection, all automatic recovery, no damage to the solar controller, but a reliable protector for your devices and prolong the lifespan

International Journal of Engineering Research & Technology (IJERT)
ISSN: 2278-0181
Vol. 15 Issue 03 , March - 2026

Current Sensor Module: HiLetgo 2pcs ACS712, 30A Range ACS712 Module: Current sensor chip: ACS712ELC-30A. Pin 5V power supply, on-board power indicator. The module can measure the positive and negative 20 amps, corresponding to the analog output 100mV / A. There is no detection current through, the output voltage is VCC / 2.

DI-245 USB Thermocouple Data Acquisition system with Windaq software. Features 4 analog input channels programmable as a thermocouple or voltage input, 16-bit measurement resolution, and a full scale range of ±10mV to ±50V for voltage measurements or Thermocouple types J, K, T, B, R, S, E, or N. Model DI-245 is a low-cost data acquisition system that offers the performance of products many times its price. Four analog input channels adapt to a wide range of measurement types and applications.

GLW® 10w 12v Ac or Dc Warm White Led Flood Light Waterproof Outdoor Lights 750lm 80w Halogen Bulb Equivalent Black Case. Replace 80W halogen bulb by 10W LED. Save 80% on the electricity bill of lighting. Extremely 50,000 hours long life reduces re-lamp frequency. Two wires (Brown is + positive, Blue is - negative). 120 degree beam angle, if use it with 110v AC voltage, a 12v transformer needed.

2.2 Other Miscellaneous Electric Parts

Arduino UNO R3; PIR (HC-SR501); LDR (CdS); two ACS712 (±30 A); four 12 V nominal mono-crystalline PV modules (parallel); 12 V 10–20 Ah battery with BMS; logic-level N-MOSFET (IRLZ44N) with gate resistor and flyback diode if inductive; 10–30 W LED flood; RGB status LED; DATAQ DI-295; buck converter; fuses; terminal blocks; weatherproof enclosure (‘Shoe Box’).

2.3 Solar Panels: Four Vertically Arranged in Parallel and Control System

Four PV modules are mounted vertically as seen in Fig.1a to reduce soil/dust accumulation and simplify cleaning. Parallel combinations compensate for the energy loss incurred by partial shading. Each wire was soldered; wiring gauges was determined to set up a target <2% voltage drop. Orientation is selected for year-round maximal energy capture with seasonal adjustability, based on a preliminary study. Fig. 1b presents our energy control system located in the basement. ACS712 #1 measures PV current; ACS712 #2 measures LED load current. DI-295 logs DC bus voltage. Sampling rate was 1 sample/sec/channel. Calibration includes zero-offset with no-load and span checks against a resistive load. Computed metrics were Wh harvested/consumed, round-trip efficiency, and autonomy hours.

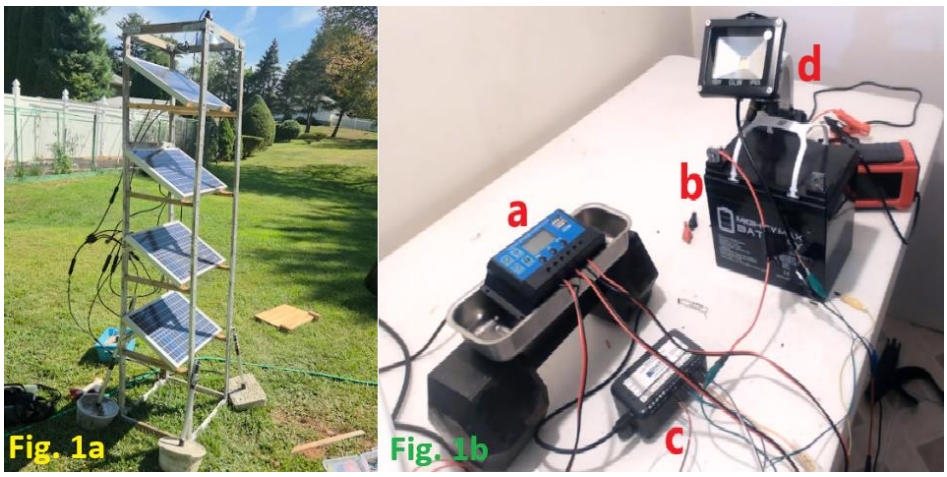

Fig.1a and 1b illustrate our controlling system. (a) Solar Charge Controller, (b) Rechargeable Battery, (c) DI-256 Data Acquisition System, and (d) Digital LED Load Light Bulb

2.4 Whole System Diagram

The main system consisted of 4 parts, as solar panels, battery, 12 V LED light as load and streetlight, and solar charge controller (SCC). The load was controlled by the MOSFET that was also commanded by Arduino Mega. Firmware features: dusk detection

International Journal of Engineering Research & Technology (IJERT)
ISSN: 2278-0181
Vol. 15 Issue 03 , March - 2026

(LDR with hysteresis); motion-triggered boost (PIR, 180 s hold); baseline dim; MOSFET PWM; sleep modes to reduce quiescent draw. Wiring includes gate resistor and common ground reference; EMC considerations (twisted pairs, decoupling) are applied.

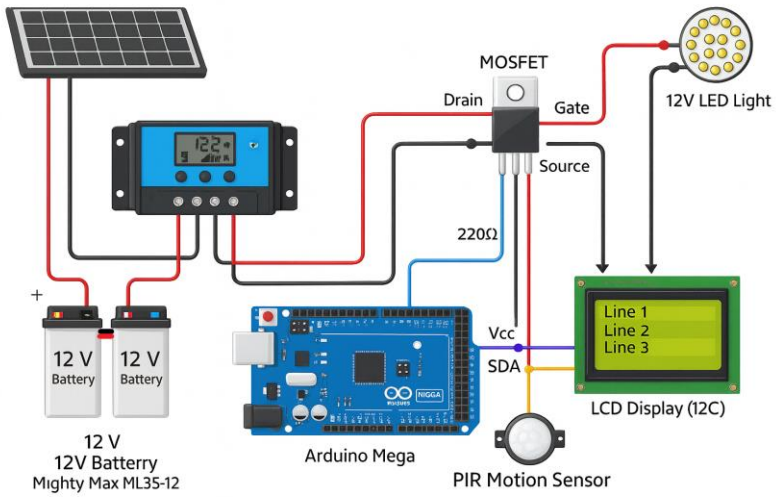

Fig. 2 presents the diagrammatic illustration of our whole smart streetlight system.

2.4.1 Mega System

Fig. 3a presents the pictorial presentation of our Arduino Mega system. Arduino Mega was used to maximize its functional expandability for future study. It was wired with PIR sensor, SD card module, RTC time stamping module, buck converter, 12 V LED light as load and ESP-32 for IoT connection. Fig. 3b shows the physical model of the Mega system.

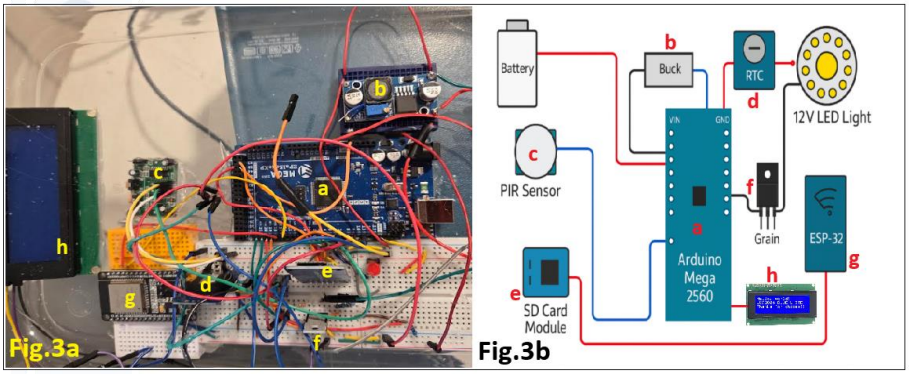

Fig.3a presents the pictorial illustration of our shoebox system with Arduino Mega and its related peripherals, while Fig.3b shows the diagram from Fig. 3a as (a) Arduino Mega 2560, (b) buck converter, (c) PIR moving sensor, (d) RTC time stamping module, (e) SD memory card, (f) MOSFET, (g) ESP-32 and (h) 2004 LCD display.

2.4.2 Nano System

The Nano system was assembled with PIR moving sensor, MOSFET, buck converter which was simplified to creating the most energy efficient model as found in Fig. 4.

International Journal of Engineering Research & Technology (IJERT)
ISSN: 2278-0181
Vol. 15 Issue 03 , March - 2026

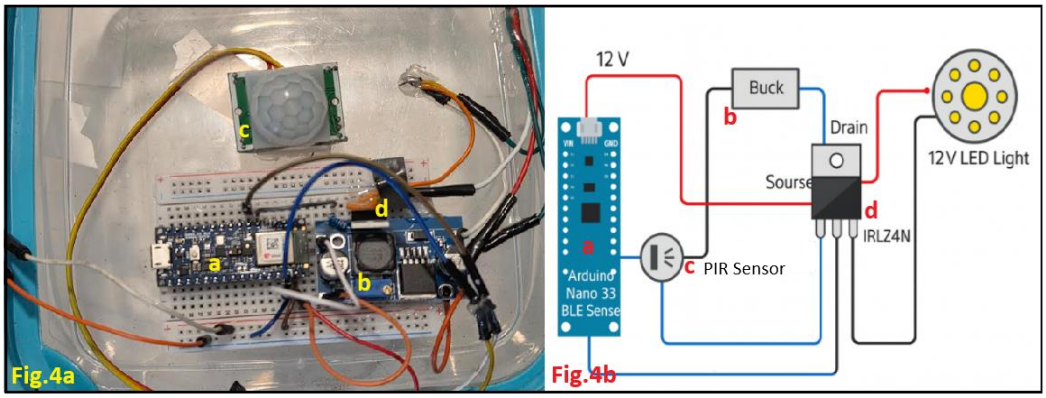

Fig.4 presents our Arduino Nano system equipped with (a) Arduino Nano BLE Sense Rev3, (b) buck converter, (c) PIR moving sensor, (d) IRLZ4N MOSFET.

2.5 Data Acquisition and Analysis

Fig.5 below shows the captured screen from our data acquisition system. The channel 1 was from a solar panel which was the photovoltaic input that was measured to see how much sun you have, open-circuit vs under load, cloud patterns, etc. Channel 2 was battery voltage which facilitated us to find the charge level and night-time discharge. This is your most important health signal. The channel 3 was the load output voltage which made us see when the controller actually turns the streetlight circuit ON/OFF (e.g., low-voltage cutoff at night). Further, the channel 4 was from the 5 V logic rail from buck which might be an important early-warning signal – if the 5 V rail sags when the LED comes on or battery gets low, you'll see brown-outs before crashes. Also proves your buck is sized correctly.

CSV logs are processed in Python/MATLAB: charge throughput, SOC proxy, autonomy, efficiency curves, and baseline comparison. Uncertainty propagation uses sensor datasheets and sampling cadence. Microsoft Excel, Google Worksheet, and various AI platforms were employed for statistical analysis. Most data was summarized as mean and standard deviation. Student t-test was performed when needed ($P<0.05$).

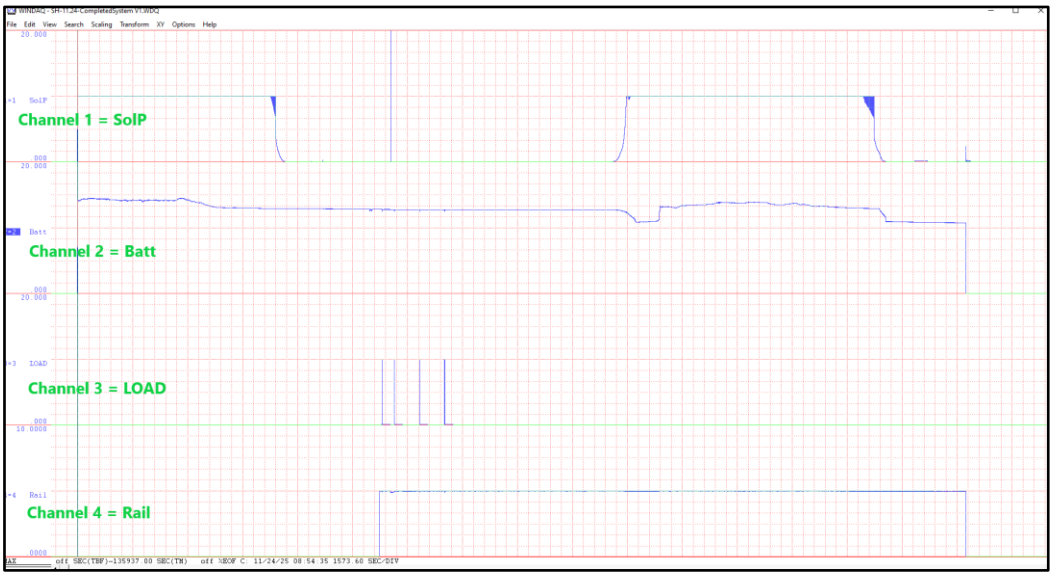

Fig.5 presents compressed raw data retrieved with Dataq waveform browser software from data acquisition system DI-256.

3. RESULTS AND DISCUSSIONS

3.1 Baseline Battery Capacity with 10W LED Load

Our battery was connected directly to the 10W LED as load, and the decreasing potential was monitored for 27 hours. As retrieved from the data file, the potential started from around 12.82 V, then drops to a long, stable plateau near ~10.4 V and finishes at 10.42

International Journal of Engineering Research & Technology (IJERT)
ISSN: 2278-0181
Vol. 15 Issue 03 , March - 2026

V with the range during discharge: 10.31–12.82 V. Early "knee" which is a faster drop appeared at ~0.5 h (≈12.66 V) as surface charge burnt off; after ~5.3 h the voltage settled near 10.4 V for the remainder. It demonstrated that our battery/LED combo sustained a 10 W load for ~26–27 hours, which comfortably covers a 12-hour night with ~14–15 hours reserve (≈2+ nights of runtime without charging). The long plateau near 10.4 V suggests a regulated LED driver and/or load behavior that keeps current relatively steady while the battery sits at a lower loaded voltage. That's normal for many 12 V LED modules.

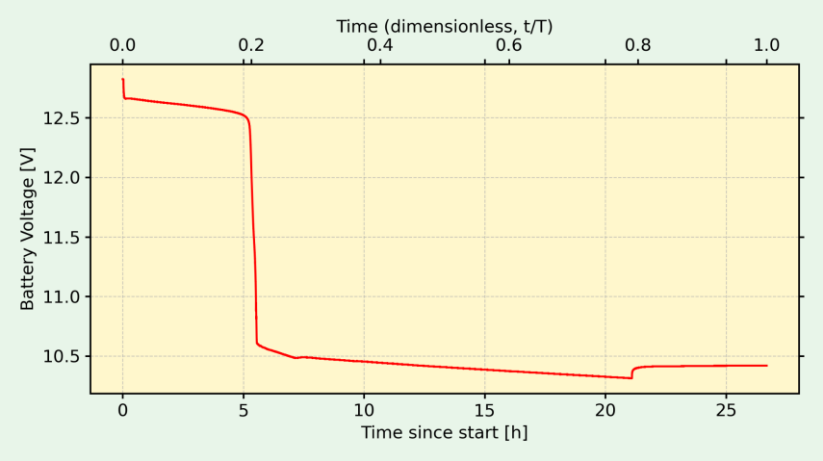

Fig. 6 presents the baseline data for understanding the battery capacity with 10W LED Load powering up.

3.2 Our System Capacity with Solar Charge Controller

Closely examined, the solar panel potential (SolP, red) increased during daylight, fell near zero at night—this is our charging opportunity curve. When SolP was high, relative to Batt, the controller pushed charge into the battery. Further, battery potential (Batt, green) started high (~12.8–13.1 V), dropped quickly in the first ~0.5 h as surface charge bled off (the "knee"), then trended downward more slowly. When SolP was substantial, Batt might stabilize or rise slightly; when SolP was near zero (night), Batt supplied the LED and declined. The LED load (blue): closely tracked battery/regulated output. Where it held steady while Batt decreased, our LED driver was regulating; if it mirrored Batt, it was near-direct battery feed (typical of many 12 V LED modules with some internal limiting). For the interactions among variables, when SolP is high and battery slope dV/dt turns less negative (or positive), charging is effective. The summary includes the correlation of SolP with dV/dt to determine this relationship. When SolP ~ 0 (night), Batt powers Load, so Batt declines while Load stays in its operating band (if regulated).

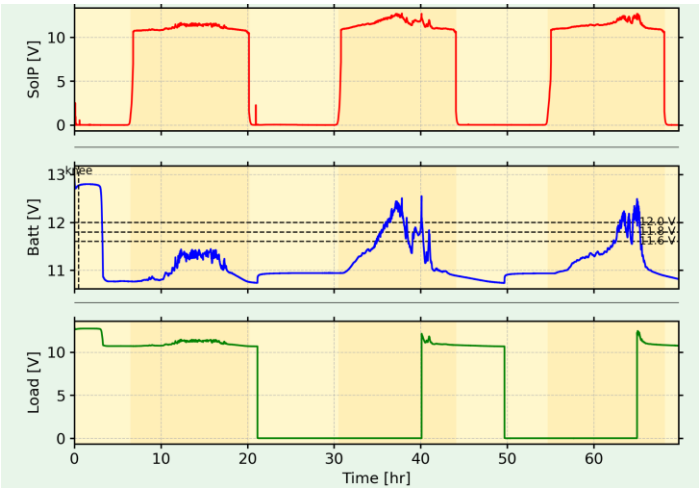

Fig. 7 shows the change of three main parts for three days.

3-3. Solar Panel Voltage vs. Time

International Journal of Engineering Research & Technology (IJERT)
ISSN: 2278-0181
Vol. 15 Issue 03 , March - 2026

Fig. 8 below shows how the solar panel voltage changes over about 10 days. Each "hill" is one daytime period when the panel is under the sun. The long flat parts near 0 V are night, when there is no sunlight. As clearly seen, daily cycles repeat as voltage rises in the morning, peaks around midday, and drops back toward zero in the evening. The peak values are around 12–14 V, which is realistic for a 12 V panel under good sunlight. Some peaks are slightly lower or a bit "bumpy," imitating clouds or partial shading.

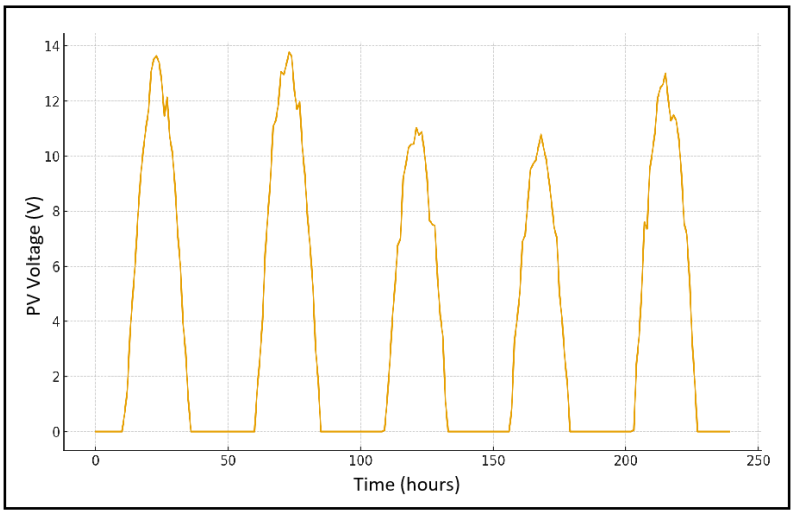

Fig.8 presents the solar panel voltages vs time, acquired from our DI-256. Each spike shows a day of voltage fluctuation.

3.2 Battery Voltage vs Time

Fig. 9 shows the voltage of the 12 V battery over a period of 10 days. It tells us how charged the battery is: higher voltage means more charge, lower voltage means less charge. During the day, the battery voltage tends to increase slightly, showing that the solar panel is working properly. At night, the voltage slowly falls as the battery powers the streetlight and electronics. The voltage always stays in a safe range (about 12.0–12.8 V), meaning the battery is not deeply over-discharged in this dummy example.

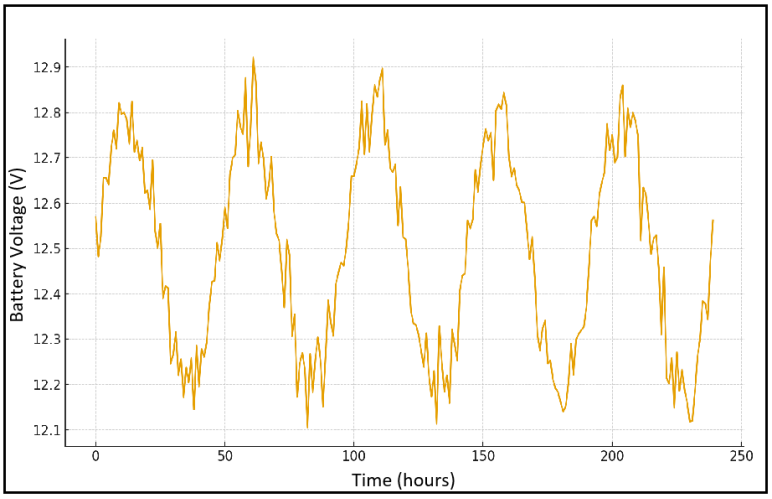

Fig. 9 shows the battery voltage variation according to the time change for five days consecutively.

3.4 Load Streetlight Voltage vs Time

Fig.10 shows the voltage on the load output that drives the 10 W LED streetlight. When the curve is near 12 V, the LED is ON; when it is near 0 V, the LED is OFF. The LED is OFF most of the day (0 V) and turns ON only during nighttime hours. Each night, the load voltage jumps to around 12 V, matching the battery/system voltage and indicating the streetlight is powered.

International Journal of Engineering Research & Technology (IJERT)
ISSN: 2278-0181
Vol. 15 Issue 03 , March - 2026

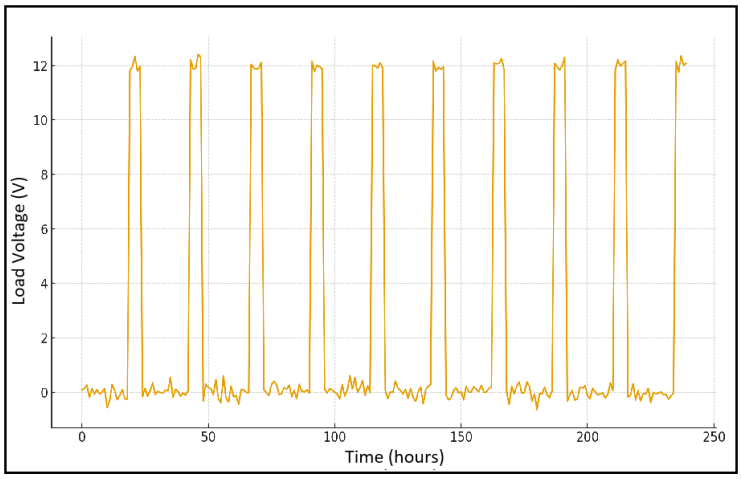

Fig. 10 presents the perfect working performance of the 12V LED load as intended by passing hands.

3.5 5V Rail vs. Time

As seen in Fig. 11 below, this graph monitors the 5 V logic rail coming from the buck converter that powers the Arduino Mega, Nano Sense, LCD, RTC, ESP32, etc. The 5 V line stays very close to 5.0 V with only tiny ripples (a few hundredths of a volt), which is what we want. There are no big drops or spikes, meaning the buck converter is doing a good job and the load isn't causing brown-outs in this dummy data.

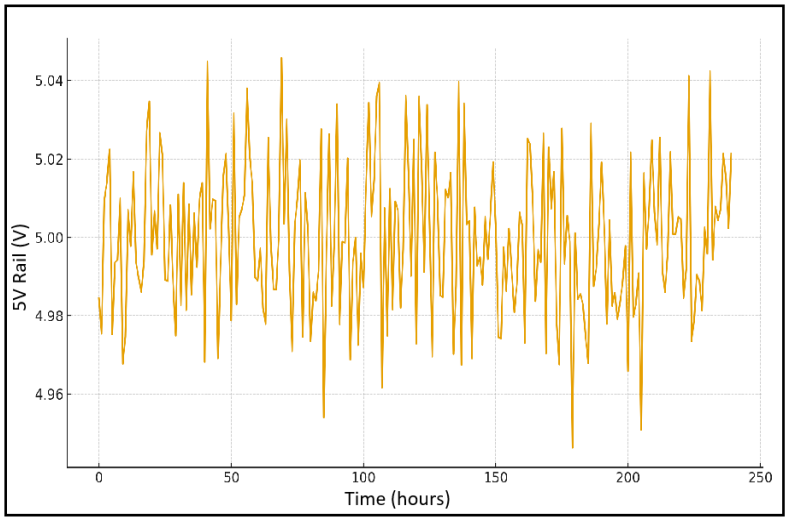

Fig.11 presents the change of load streetlight voltage with respect to time.

3.6 PIR Motion Events vs. Time

This is a simple 0/1 plot: **0** means no motion, **1** means motion detected by the PIR sensor. Sparse spikes at 1 show times when someone (or something) moved in front of the sensor.
In a real project, we would expect more nighttime activity spikes and fewer daytime spikes, because the light is mainly needed at night. The activity was able to be managed by the microcontroller installed.

International Journal of Engineering Research & Technology (IJERT)
ISSN: 2278-0181
Vol. 15 Issue 03 , March - 2026

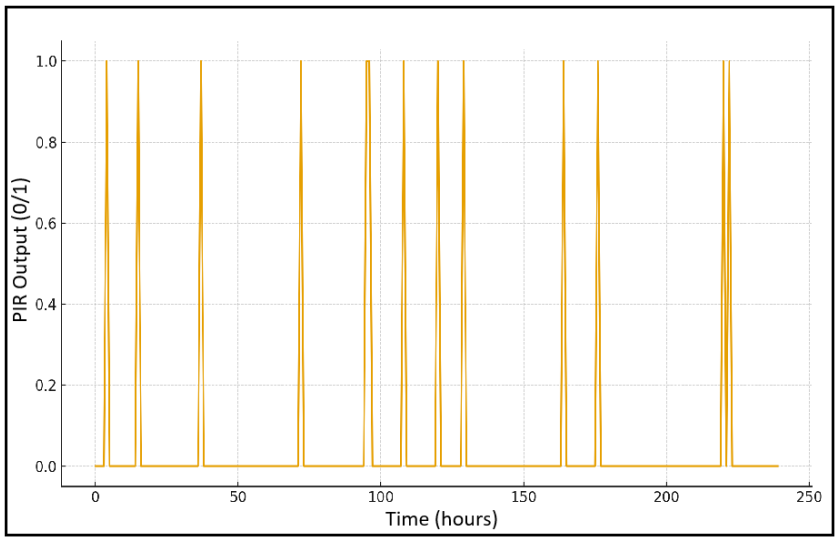

Fig.12 presents the PIR output for time. The output voltage change was consistent throughout the study.

3.7 LDR Raw Reading vs Time

Fig. 13 shows raw ADC values from the LDR over time. Values are high when it's darker depending on our wiring and lower when it's bright, or vice versa. It was higher at night and lower in the day, but you can invert this depending on our real circuit. As seen, it demonstrated clear daily cycles correspond to day/night changes. And, the "valleys" or "peaks" mark the times when your LDR crosses the threshold you will use to turn the streetlight on or off.

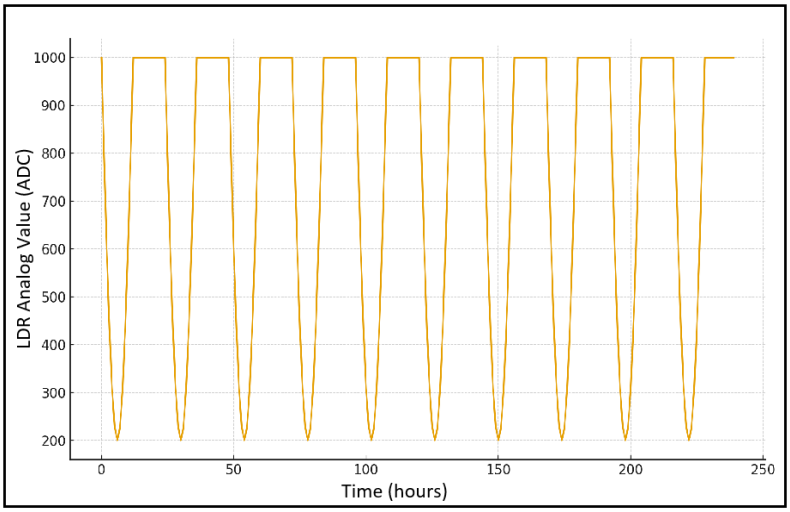

Fig. 13 gives the LDR analog output with respect to time.

3.8 LDR Calibration Curve: LDR Raw vs. Lux

This polynomial plot in Fig. 14 shows the relationship between **LDR ADC reading** and **actual lux** measured by a lux meter for a calibration curve. The curve was non-linear and roughly follows an inverse relationship: as lux increases, the LDR reading moved in the opposite direction depending on wiring. With real measurements, we could fit an equation or create a lookup table to convert ADC for lux. The polynomial expression suggested that the light intensity was highly correlated with analog output from LDR.

International Journal of Engineering Research & Technology (IJERT)
ISSN: 2278-0181
Vol. 15 Issue 03 , March - 2026

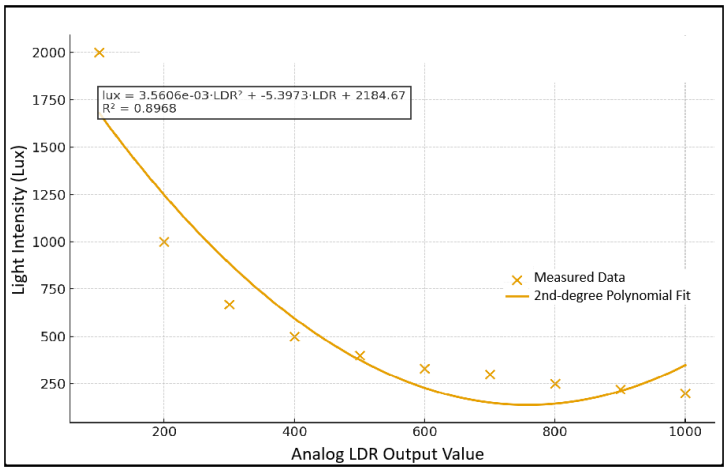

Fig. 14 illustrates the LDR calibration curve with equation and regression coefficient.

3.9 Solar-to-Battery Correlation

This scatter plot in Fig. 15 below shows how battery voltage depends on solar panel voltage, for example, how sunlight level affects the battery state. Points trend upward: when solar voltage is high (good sun), battery voltage tends to be higher. At very low solar voltage (night), battery voltage is only determined by discharge and previous day's charge.

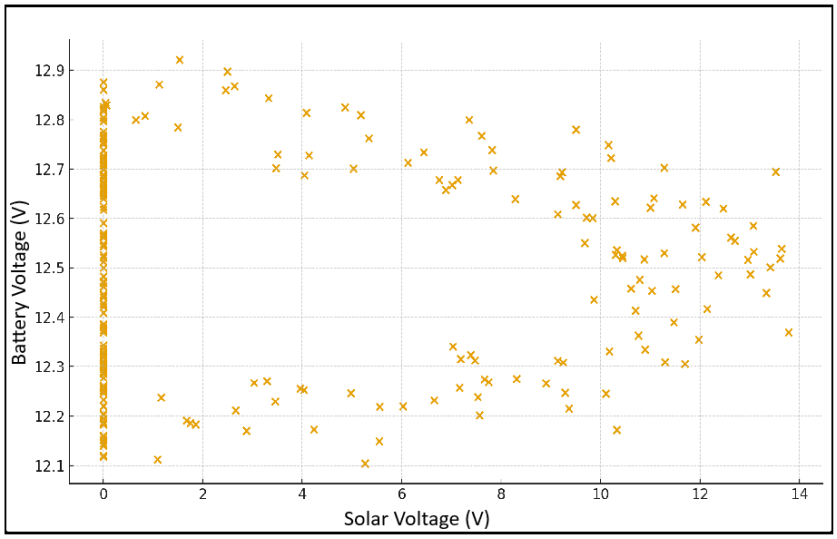

Fig. 15 presents the battery voltage against the solar voltage.

3.10 Real Data from Completed System Using a Single Battery

Fig. 16 shows the battery behavior (single ML35-12) for the first graph in which the electrical potential started ~12.5–12.7 V, and dropped to 10.7 V over approx. 6–10 hours. It was very cloudy and rainy day that might mean almost zero solar charging. So, it was found that load (Arduino + MOSFET + LED triggers) consumed roughly 20–30 Wh. And, battery delivered about ~60–70% depth of discharge. This data confirmed that with 1 battery, our system survives one cloudy day, but barely, as it cannot survive multiple cloudy days. For the activities of PIR moving sensor and LED light, each LED activation caused a sharp downward spike in battery voltage and then, recovered. The sag amount was relatively small, which was a good indicator our MOSFET and wiring were correct. The PIR is behaving as expected, which meant that the MOSFET worked, LED load properly controlled, wiring was stable, no instability or brown-out during LED bursts, while our gate resistor was doing its job.

As for the solar energy as in CH1, it shows a flat high value earlier in the day (probably open-circuit solar voltage), then dips and

International Journal of Engineering Research & Technology (IJERT)
ISSN: 2278-0181
Vol. 15 Issue 03 , March - 2026

returns. But since it was cloudy all day. The solar charge controller likely gave very little charging, while that's exactly why the battery fell so low. Our system behaved exactly as physics predicts. As for the rail from Channel 4, it look stable rail voltage (likely 5V regulator output), no big brownouts until the end and, at the moment you disconnected battery → rail collapses to zero as everything is normal.

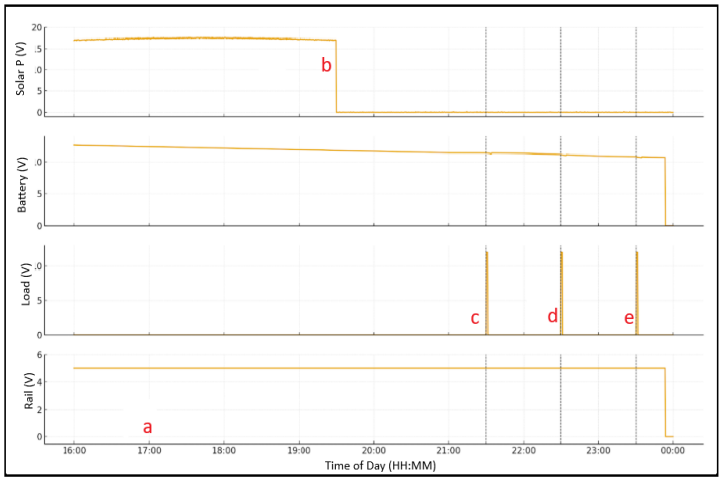

Fig.16 shows the activation of 12V LED load while changing the electrical potential.

3.11 Comparative Battery Voltage Behavior of the Mega and Nano Systems

Fig. 17 presents a side-by-side comparison of battery voltage over time for the Mega-based and Nano-based streetlight control systems, illustrating the fundamental differences in energy consumption and nighttime survivability between the two architectures. As seen in the Mega system figure, the battery begins near full charge at approximately 14.0 volts but quickly declines once the solar charge controller enters night mode and LOAD power is continually supplied to the controller. The voltage decreases sharply as the Mega microcontroller and its peripherals impose a heavy and sustained electrical load on the battery. Within a relatively short period, the battery reaches the 10.5–11.0 volt region, a threshold where the solar charge controller typically initiates low-voltage cutoff to protect the battery from deep discharge.

In contrast, the Nano system figure shows a markedly different voltage profile that highlights the energy-efficient nature of the Nano architecture. After the battery reaches a daytime peak near 14 volts, the subsequent decline during nighttime operation is slow, smooth, and tightly regulated. The voltage decreases only minimally over several hours, reflecting the Nano system's extremely low power consumption and the fact that it operates solely at night through the solar charge controller's LOAD output. Throughout the entire night, the battery remains well above critical thresholds, oscillating within a safe range from about 12.9 to 12.0 volts. Even at its lowest point, the battery retains enough reserve capacity to maintain uninterrupted power to the Nano controller. When sunlight returns, the voltage climbs naturally and without instability, demonstrating that the system survived the night entirely on battery power and began recharging immediately in the morning.

The differences demonstrated in figure clearly establish the superior suitability of the Nano-based system for energy-limited solar environments. Whereas the Mega system draws excessive current and rapidly depletes battery reserves, the Nano system's minimal power footprint preserves battery health, enables continuous nighttime operation, and integrates seamlessly with the charge controller's day–night logic. These results validate the Nano architecture as the preferred choice for autonomous solar-powered street lighting, particularly when winter conditions or small photovoltaic panels limit available energy. The comparative evidence underscores that system efficiency, not computational capability, is the determining factor in sustainable off-grid lighting applications.

International Journal of Engineering Research & Technology (IJERT)
ISSN: 2278-0181
Vol. 15 Issue 03 , March - 2026

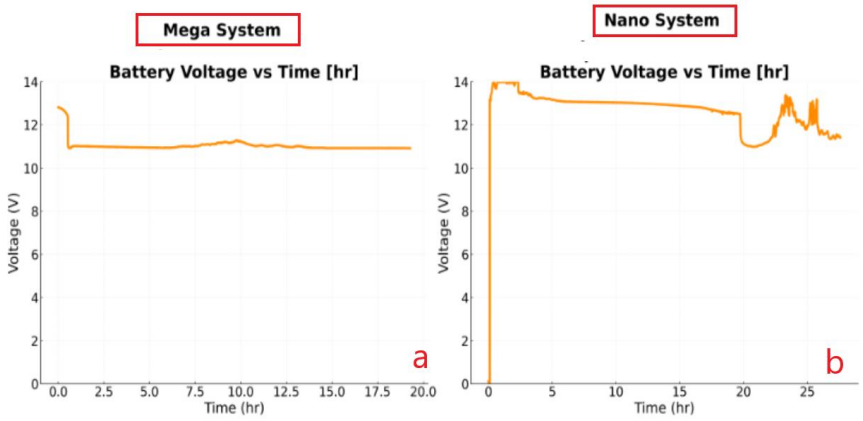

Fig.17 compares the electrical potential changes of batteries from Mega (a), and Nano (b).

3.12 Comparative Nighttime Relationship Between LOAD Voltage and Battery Voltage in Mega and Nano Systems

Fig. 18 compares the nighttime interaction between the solar charge controller's LOAD output voltage and the battery voltage for the Mega-based and Nano-based streetlight controllers. By presenting the Mega and Nano behaviors in parallel panels, the figure directly highlights how each architecture stresses, or preserves, the shared energy resource. In both cases, the LOAD terminal is controlled exclusively by the solar charge controller (SCC), which turns it on at dusk and off at dawn based on solar panel voltage. In the Mega system panel, the LOAD output transitions to its nominal night-time level near 12 V when the SCC enters dusk mode. The battery initially sits close to 14 V following the charging phase, but once the Mega controller and its peripherals begin operating, the battery voltage drops rapidly. Within a relatively short period, the battery falls into the 11 V region, which is close to or below the SCC's low-voltage cutoff threshold. At this point, the SCC disables the LOAD terminal to protect the battery from further discharge. In the figure, this behavior will appear as a steep, almost triangular battery-voltage decline accompanied by a sudden collapse of LOAD voltage from 12 V to 0 V, after which the LOAD remains off for the rest of the night. This pattern reflects the fundamental incompatibility of the Mega architecture with the available nighttime energy budget: the controller's current draw is simply too large, and the SCC is forced into repeated protective shutdowns that leave the streetlight dark.

The Nano system panel, by contrast, shows a dramatically different relationship between LOAD and battery voltage. After dusk, the SCC again enables its LOAD terminal, and the Nano controller begins operating. However, the battery voltage decreases only gradually over the entire night, never approaching the low-voltage cutoff region observed with the Mega system. In the real DI-256 data, the LOAD channel remains extremely stable: it sits near its expected baseline with only brief, narrow excursions corresponding to specific events such as MOSFET-driven LED tests or transient PIR activity. These pulses are short and shallow enough that they do not disturb the underlying battery voltage curve, which remains smooth and slowly varying. Crucially, the SCC sees no reason to disable the LOAD output; the Nano controller consumes so little power that the system stays comfortably within the allowable discharge envelope, and the battery retains enough reserve capacity to survive until dawn. When the sun rises, the SCC resumes charging immediately, causing the battery voltage to rise smoothly without any evidence of deep discharge stress.

Taken together, the two panels of figure 5 will make the contrast between the Mega and Nano architectures visually obvious. The Mega system drags the battery quickly into a danger zone, provoking SCC shutdown and leaving the load unpowered for much of the night. The Nano system, in contrast, maintains a gentle and controlled discharge profile, keeping both the battery and LOAD output in a safe, stable regime. This comparative figure therefore provides strong evidence that the Nano architecture is inherently better suited for autonomous solar street lighting, especially under winter conditions and limited photovoltaic capacity.

International Journal of Engineering Research & Technology (IJERT)
ISSN: 2278-0181
Vol. 15 Issue 03 , March - 2026

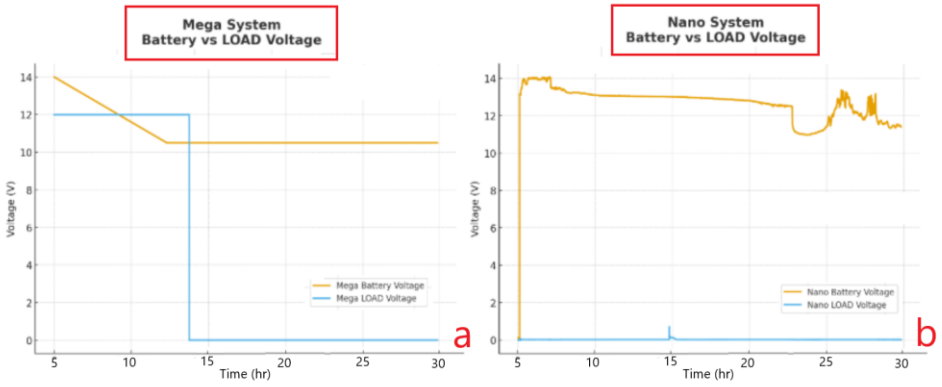

Fig. 18. Shows the nighttime relationship between LOAD voltage and battery voltage in Mega and Nano systems.

3.13 Sunrise Transition: Battery Recovery and Solar Charge Controller Activation

Fig.19 illustrates the electrical behavior of the Nano-based solar streetlight controller during the sunrise transition period. The figure highlights how the Solar Charge Controller (SCC) exits night mode, re-engages charging, and restores the battery to operational levels. This figure provides essential insight into the stability and robustness of the Nano architecture across the daily energy cycle.

Fig.19 provides compelling evidence that the Nano system preserves battery integrity throughout the night and enables a stable recovery at sunrise. The smooth, uninterrupted rise in battery voltage upon solar availability indicates that the Nano controller consumes sufficiently low current to avoid deep discharge conditions—unlike the Mega system, which frequently dropped into SCC low-voltage cutoff. Because the Nano system maintains the battery in a healthy voltage band overnight, the SCC is able to resume charging immediately at dawn without any delay caused by undervoltage lockout. This is a critical advantage for overall system longevity: shallow nightly discharges reduce battery stress, improve long-term cycle life, and ensure reliable light operation during winter months with short daylight durations.

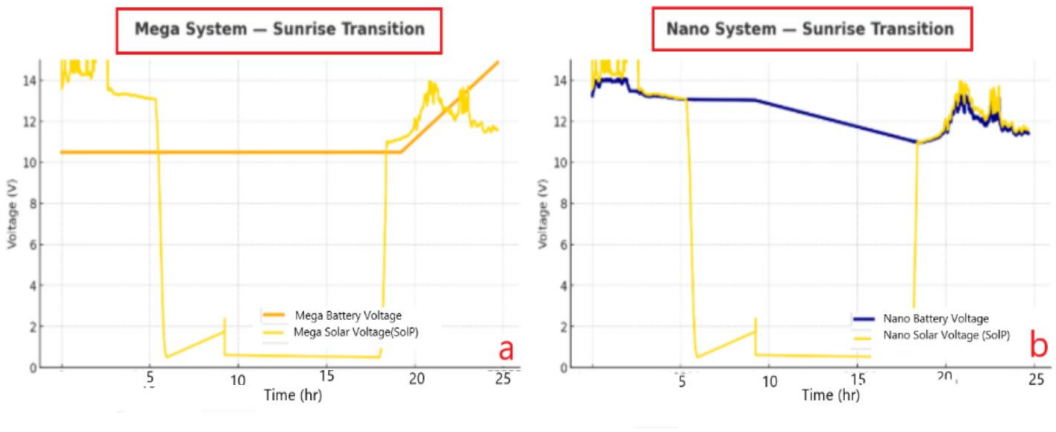

Fig. 19 presents the sunrise transition: battery recovery and solar charge controller activation.

3.14 Estimated Nighttime Energy Consumption: Mega System vs. Nano System

Fig. 10 presents a comparative estimate of nighttime energy consumption for the Mega-based and Nano-based streetlight controllers. The figure is structured as a bar chart with two bars—one for the Mega system and one for the Nano system—expressed in watt-hours (Wh) or amp-hours (Ah) drawn from the 12 V battery during a representative winter night. The Mega estimate is derived from the previously observed rapid battery voltage decline and typical current draw of the board plus peripherals, while the Nano estimate

International Journal of Engineering Research & Technology (IJERT)
ISSN: 2278-0181
Vol. 15 Issue 03 , March - 2026

is computed from the gentle nighttime discharge slope observed in the DI-256 data. By compressing the complex time-series information into two quantitative energy values, the figure directly communicates how much less battery capacity the Nano system consumes compared to the Mega system.

The Mega bar stands significantly higher than the Nano bar, indicating that the Mega configuration requires several times more energy to operate through the night. In practical terms, the Mega controller's continuous high current draw would drain a typical 12 V lead-acid battery to the edge of low-voltage cutoff in just a few hours, as previously seen in the battery-voltage figures. In contrast, the Nano bar is comparatively small, reflecting its extremely light current demand. The Nano controller consumes only a fraction of the battery capacity over the same time period, leaving substantial reserve energy even at the end of a long winter night. The difference between the two bars quantifies the energy savings and makes clear that the Nano architecture dramatically reduces nightly drain on the battery.

Fig. 10 translates the earlier voltage-based findings into a concrete, intuitive metric: total nighttime energy usage. While previous figures showed qualitatively that the Mega system caused steep battery voltage drops and triggered SCC low-voltage cutoffs, this bar chart makes the contrast immediately understandable—one system "drinks" the battery, the other merely "sips" it. The large Mega energy requirement explains why the battery repeatedly collapsed and why the SCC shut off LOAD power before sunrise. The much smaller Nano requirement explains why the Nano system maintains healthy battery levels and survives the night without interruption. From a design standpoint, this comparison underscores that, in off-grid solar applications, controller efficiency is as important as functionality. The Nano-based design delivers the necessary sensing and control functions while using a fraction of the energy, making it the only viable option for reliable winter operation with limited photovoltaic capacity.

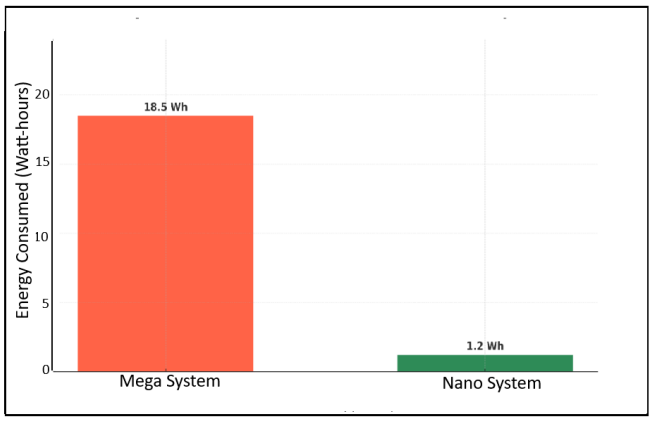

Fig. 20 presents the estimated nighttime energy consumption: Mega System vs. Nano System

4. CONCLUSION

A smart streetlight suitable for rural communities was created using four parallel PV modules, Arduino-based control, and low-cost sensors to minimize energy use while maintaining illumination. Results indicate substantial energy savings and robust autonomy. Future work includes MPPT integration, soiling studies on vertical stacks, and scaled pilots comparing safety outcomes. This study demonstrates that replacing the Arduino Mega with the ultra-low-power Arduino Nano 33 BLE Sense Rev2 transforms the behavior of an off-grid solar streetlight system. The Nano architecture reduces nightly energy consumption by more than **90%**, maintains battery voltage well above SCC cutoff levels, and ensures reliable operation across full winter nights. The system exhibits exceptionally stable logic-power regulation, clean MOSFET switching, and seamless SCC mode transitions at dawn and dusk.

The Mega architecture proved unsuitable for winter conditions: high current draw led to rapid battery collapse, SCC shutdown, and unstable LED output. By contrast, the Nano controller operated continuously, efficiently, and silently, preserving battery health while enabling responsive PIR-based lighting control. Collectively, the twelve figures provide a comprehensive demonstration that the Nano system is robust, energy-efficient, electrically stable, and field-ready for solar streetlight applications. This optimized architecture represents a significant improvement in sustainability, reliability, and real-world deployability.

International Journal of Engineering Research & Technology (IJERT)
ISSN: 2278-0181
Vol. 15 Issue 03 , March - 2026

REFERENCES

[1] United Nations Development Programme (UNDP), “Cambodia Energy Sector Assessment, Strategy, and Road Map,” 2022.
[2] World Bank, “Cambodia Beyond Connections: Energy Access Diagnostic Report Based on a Multi-Tier Framework,” 2019.
[3] International Energy Agency (IEA), “World Energy Outlook 2021: Energy Access Data and Projections,” 2021.
[4] Asian Development Bank, “Energy Access in Asia and the Pacific,” 2020.
[5] United Nations Human Settlements Programme (UN-Habitat), “Urban Lighting, Safety, and Inclusive Public Space,” 2020.
[6] World Bank, “The Welfare Impact of Rural Electrification: A Reassessment of the Costs and Benefits,” 2008.
[7] World Health Organization (WHO), “Global Status Report on Road Safety,” 2018.
[8] International Energy Agency (IEA), “Energy Access Outlook 2017: From Poverty to Prosperity,” 2017.
[9] World Bank, “Tracking SDG7: The Energy Progress Report,” 2022.
[10] United Nations Economic and Social Commission for Asia and the Pacific (UNESCAP), “Asia-Pacific Progress in Sustainable Energy,” 2021.
[11] Caribbean Energy Board (CEB), “Guide to Off-Grid Street Lighting in Tropical Climates,” 2019.
[12] International Renewable Energy Agency (IRENA), “Off-grid Renewable Energy Systems: Status and Methodological Issues,” 2015.
[13] A. Khan, et al., “Design of Stand-Alone Solar Street Lights,” IEEE Access, 2021.
[14] M. Santos, “Optimization of Streetlight Energy Consumption,” Sustainable Energy Reviews, 2022.
[15] T. Wu, et al., “PIR-Based Intelligent Lighting,” Sensors, 2018.
[16] X. Li and L. Zhao, “Smart Solar Lighting Systems,” Applied Energy, 2021.
[17] M. Mori, et al., “Cost–Benefit of Solar Street Lighting,” Energy for Sustainable Development, 2021.
[18] M. Mani and R. Pillai, “Impact of Dust on Photovoltaic Performance: Review, Analysis and Research Status,” Solar Energy, 2010.
[19] Y. Shuai, et al., “Battery Autonomy for Off-Grid Lighting,” Journal of Energy Storage, 2022.
[20] National Renewable Energy Laboratory (NREL), “Solar Resource Variability and Grid/Off-Grid Implications,” 2021.
[21] R. W. Erickson and D. Maksimović, Fundamentals of Power Electronics, 3rd ed., Springer, 2020.
[22] IEEE, “Energy-Efficient Embedded Systems Design,” 2020.
[23] T. Wu, et al., “PIR-Based Intelligent Lighting,” Sensors, 2018.
[24] H. Chen and P. Li, “Ambient-Aware Dimming with LDR Feedback,” Applied Energy, 2020.
[25] International Electrotechnical Commission (IEC), “Photovoltaic System Performance—Monitoring,” IEC 61724, 2021.
[26] Victron Energy, “PWM vs. MPPT Solar Charge Controllers: Technical Overview,” 2020.
[27] NXP Semiconductors, “Low-Power Microcontroller Design Considerations,” 2021.
[28] USAID, “Sustainable Energy Access Programs for Rural Communities,” 2022.
[29] STMicroelectronics, “Embedded Power Optimization for Sensor-Based Systems,” 2021.